Int. J. Solids Structures Vol. 15, pp. 15–31

0020-7683/79/0101-0015/$02.00/0

LARGE VISCOPLASTIC DEFLECTIONS OF IMPULSIVELY LOADED PLANE FRAMES†

P. S. SYMONDS‡ and C. T. CHON§

Division of Engineering, Brown University, Providence, RI 02912, U.S.A.

(*Received* 27 *December* 1977; *in revised form* 5 *June* 1978)

Abstract—Applications are described of two estimation techniques to obtain final deflections and response times of plane rectangular frames subjected to impulsive loading on the transverse (beam) member. Deflections up to roughly one third the span (thirty thicknesses) are estimated by the mode approximation and deflection bounds techniques, treating the plastic rate dependence by means of homogeneous viscous constitutive equations. Comparisons are made with recent test results, and the degree of agreement is discussed in terms of the known error sources of the two techniques.

1. INTRODUCTION

The impulsively loaded plane frame considered here is assumed to exhibit strong plastic rate sensitivity and to reach large deflections. We shall describe applications of the mode approximation technique and of the deflection bound method to this type of structure. Experiments intended to check on these methods are described in a companion paper[1]. The comparison between predictions of the estimation techniques and the test results is discussed in order to assess the relative importance of the intrinsic errors of the methods, and those due to further idealizations and approximations made in their application to this type of structure.

The two types of frames considered are shown in Fig. 1. Type (a) in Fig. 1(a) has a concentrated impulse applied to a small block at the midpoint of the beam (transverse) member, while type (b) in Fig. 1(b) has a distributed impulse applied over this member. These loads are idealized as impulsive (zero duration), imparting specified initial velocities with negligible initial displacements. Symmetric deformations are expected, the main displacement magnitude being the displacement at the midpoint C of the beam member. At large deflections such as indicated in Fig. 2(b), a finite lateral displacement occurs at the top B of each column. The particular frames studied here and in the related tests had lengths $L_1 = 5.625$ in. in the case of the "type (a)" frames, $L_1 = 6.00$ in. for the type (b) frames, with $L_2 = 8.00$ in. in both cases. Two strongly rate-sensitive metals, mild steel and commercially pure titanium were used. In these circumstances the large deflections have primarily kinematic effects, without requiring drastic changes in the stress field; the response remains primarily flexural.

2. BASIC CONCEPTS AND EQUATIONS

The essential concepts of the two techniques will be outlined briefly. Further information on the approaches may be found for the bound method in[2, 3] and for the extended mode approximation technique in[3, 4].

The deflection bound method for a structure of viscoplastic material, subjected to impulsive pressures at $t \leqslant 0$ and thereafter unloaded, requires the solution for quasi-static deflections due to a certain concentrated force P^s_{An}: if the deflection is sought at point A of the structure (located by appropriate coordinates x_A) in direction **n** (a unit vector), P^s_{An} is applied at this point and in this direction. If the force P^s_{An} is such that it does work at least equal to the specified initial kinetic energy of the structure, then the displacement on which it does work is an upper bound on the same deflection quantity in the response to the given dynamic loading. If t_f is the time at which the plastic deformation is completed, the theorem requires the work of the force

†Research supported by National Science Foundation under Grant ENG74-21258 and by Office of Naval Research under Contract N00014-75-C-0860.

‡Professor of Engineering, Brown University.

§Research Associate, Brown University. Now at: Research Laboratory, General Motors Corporation, Warren, Michigan, U.S.A.

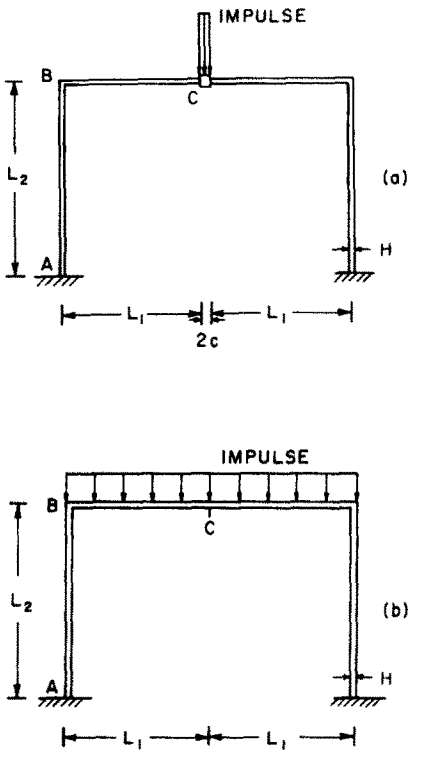

Fig. 1.

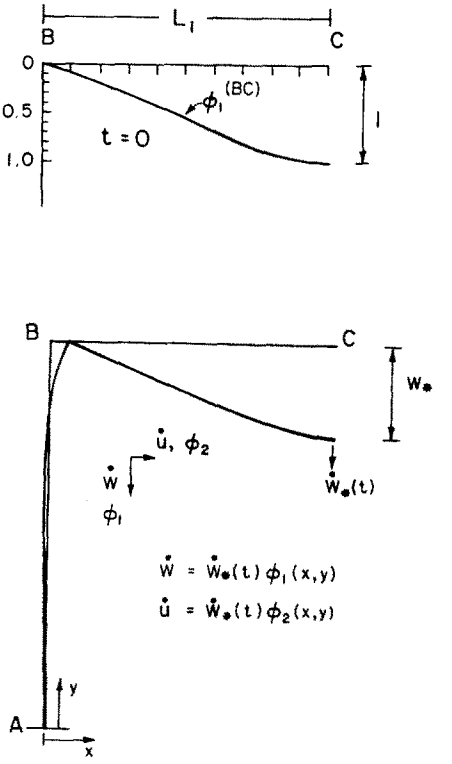

Fig. 2.

Fig. 1. Frame types considered here and in experiments[1]. Type (a) has steel block at midpoint of transverse member, type (b) has uniform transverse member.

Fig. 2. Notation for mode form solution.

P^s_{An} to be done in time t_f. (For a time-dependent material the work to reach specified final strains depends on the time in which they are reached.)

In mathematical terms the bound theorem states that

$$u^f_{An} \leq u^{sf}_{An} \tag{1a}$$

where u^f_{An} is the final displacement at point A in direction n of the dynamically loaded structure, reached at time t_f; and u^{sf}_{An} the displacement at time t_f due to the static force P^s_{An}; the inequality holds provided

$$K_0 \leq \int_V \dot{W}(q^{sf}_j)\,\mathrm{d}V \tag{1b}$$

where K_0 is the initial kinetic energy of the impulsively loaded structure and the r.h.s. represents the work done by the force P^S_{An} in the interval of time $0 \leq t \leq t_f$; $\dot{W}(q^{sf}_j)$ denotes work per unit volume written as function of the terminal generalized strains q^{sf}_j, $j = 1, .. r$, for generalized strain and stress states having r components.

As noted above, this work depends on the interval t_f. Generally it also depends on the path, i.e. on the sequence of strain states from the initial to the terminal. We have eliminated path dependence by using concepts of minimum work paths[2, 3], $\dot{W}$ denoting the work per unit volume which is a minimum for given terminal strain. The total work is evaluated as

$$\int_V \dot{W}\,\mathrm{d}V = n\left(\frac{n}{n+1}\right)^n t_f \int_V \psi(Q^{sf}_j)\,\mathrm{d}V \tag{1c}$$

where $\psi(Q^{sf}_j)$ is a homogeneous function of terminal stresses Q^{sf}_j, whose degree of homo-

geneity is $n+1$. More generally, the function ψ furnishes constitutive equations relating stress to strain rate states in a convenient form, from the property

$$\dot{q}_j = \frac{\partial \psi}{\partial Q_j} \tag{2}$$

where $\dot{q}_j$ are strain rate components.

The "intrinsic error" of the deflection bound is positive: an *upper* bound is obtained. In this statement the comparison is made between a computed quasistatic deflection according to a certain mathematical model, and a deflection resulting from impulsive loading on the structure represented by the same model. When comparison is made instead with the final deflection of an actual structure as opposed to a mathematical model, the idealizations and approximations adopted in the calculation of u_n^* may introduce further errors. Some of the idealizations are indicated above; they will be discussed with others more fully in a later section. Obviously the aim is to make the calculation in such a way that the incidental errors are minor compared to the intrinsic ones. The need for comparisons with experiments rather than merely with computer outputs is also obvious.

The essential concept of the mode technique is that of obtaining an approximation to the actual response from a simpler solution which satisfies all the field equations (dynamics, kinematics including boundary fixing conditions, and constitutive equations), but disagrees in general with the imposed initial velocities. Such simpler solutions can be found under certain conditions in modal form, with velocity field, for example, written as

$$\dot{u}_i^*(x, t) = T(t)\phi_i(x) \tag{3}$$

where $i = 1, 2, 3$; $T(t)$ is a scalar function of time t; and $\phi_i(x)$ is a vector-valued function of space coordinates x. The initial velocities

$$\dot{u}_i^*(x, 0) = T_0\phi_i(x) \tag{4}$$

where $T_0 = T(0)$, usually differ from the velocities specified at $t = 0$, namely

$$\dot{u}_i(x, 0) = u_i^0(x) \tag{5}$$

since the shape functions $\phi_i(x)$ are properties of the structure. However the initial magnitude T_0 can be chosen optimally by taking[5]

$$T_0 = \int_V \rho \dot{u}_i^0 \phi_i \, dV \Big/ \int_V \rho \phi_i \phi_i \, dV \tag{6}$$

where ρ is the mass density and the integral is over the volume V of the structure. This value of T_0 minimizes the initial magnitude of the following functional:

$$\Delta(t) = \Delta[\dot{u}_i(x, t) - \dot{u}_i^*(x, t)] = \frac{1}{2}\int_V \rho(\dot{u}_i - \dot{u}_i^*)(\dot{u}_i - \dot{u}_i^*) \, dV. \tag{7}$$

It has been shown[6] for a wide class of material behavior of essentially viscous type (generalized strain rates written as functions of generalized stress), (and assuming small deflections) that $\Delta(t)$ is a non-increasing function, which decreases whenever plastic flow occurs and the two solutions do not have identical stresses or strain rates. Thus the actual velocity field and that of the mode solution approach each other in this sense. With T_0 chosen according to eqn (6), the two solutions may become identical after a certain interval. The final major displacement computed from the mode solution is therefore usually much closer to that of the structure than the initial mode amplitude is to the corresponding given initial velocity.

The final major deflection of the mode response will be greater or less than that of the structure whose initial velocity is the specified one, depending on whether the initial mode

velocity field is more or less concentrated than the given velocity distribution. This intrinsic error evidently can be positive or negative. Here again the "error" refers to quantities computed using a certain mathematical model to represent a structure. The calculation of the mode response involves idealizations and approximations, and when the results are compared with deflections and response times of a real structure, further errors may appear. These will be discussed in a later section.

The mode method requires the integration of the equations of the structure, from the initial mode form velocity field to the end of the motion. This integration presents no difficulty if the equations allow the separated-variable form of eqn (3) to hold during the entire response. If small-deflection equations are not used, such "permanent" mode solutions do not exist. A convenient way of performing the integration in these cases is by means of a sequence of "instantaneous" mode form solutions [3, 4]. At finite deflections the solution can be put in the form of eqn (3) if the deflection is regarded as instantaneously fixed and known. Thus the instantaneous shape function $\phi_i(x)$ changes during the response and may be written as $\overset{\langle t \rangle}{\phi_i}(x)$. Successive "solutions" in this form are linked through equations of the form

$$u_i(x, t_{n+1}) = u_i(x, t_n) + \frac{\Delta t}{2}\left[T(t_n)\overset{\langle t_n \rangle}{\phi_i}(x) + T(t_{n+1})\overset{\langle t_{n+1} \rangle}{\phi_i}(x)\right] \tag{8a}$$

$$T(t_{n+1}) = T(t_n) + \frac{\Delta t}{2}\left[\dot{T}(t_n) + \dot{T}(t_{n+1})\right]. \tag{8b}$$

This method is not exact, even though the field equations are instantaneously satisfied; the mode solution has a smaller energy dissipation rate than the actual motion at the same level of kinetic energy [7]. This method may be expected to lead to a response of longer duration and larger deflections than the actual motion of the structure would be under the same starting conditions, so that the approximation due to this device for carrying out the integration for large deflections is therefore expected to be conservative.

Here we write the equations used in both the mode technique and the deflection bound method; the dynamical equations for the latter are obtained by setting the accelerations equal to zero.

The notation is indicated in Fig. 2(b). We use rectangular coordinates x, y with origin at the base A of the left-hand column. Velocity components are shown in Fig. 2(b). Nondimensional quantities are used, defined as follows

$$x = \frac{\bar{x}}{L_1}, \qquad y = \frac{\bar{y}}{L_2}, \qquad t = \frac{\bar{t}}{\tau} \tag{9a}$$

$$u = \frac{\bar{u}}{H}, \qquad w = \frac{\bar{w}}{H}, \qquad \dot{u} = \frac{\tau}{H}\frac{\partial \bar{u}}{\partial \bar{t}}, \qquad \dot{w} = \frac{\tau}{H}\frac{\partial \bar{w}}{\partial \bar{t}} \tag{9b}$$

where $\bar{x}$, $\bar{y}$; $\bar{t}$; $\bar{u}$, $\bar{w}$ are coordinates, time, and displacements in physical units, H is thickness, and $\tau = 2L_1\sqrt{(\rho/\sigma_0)}$ is a reference time, ρ being mass density and σ_0 being a stress property obtained from tests on strain rate dependent plastic behavior, as defined more fully below. For general stress and strain states in a one-dimensional structure, relations between bending moment, axial force and the corresponding strain rates are required. We take the viscoplastic behavior to be expressible in the form

$$\frac{\sigma}{\sigma_0} = 1 + \left(\frac{\dot{\epsilon}}{\dot{\epsilon}_0}\right)^{1/n}, \quad \dot{\epsilon} > 0 \tag{10}$$

where σ, $\dot{\epsilon}$ are uniaxial stress and plastic strain rate, respectively, corresponding (in general) to a fixed level of plastic strain ϵ^p; and σ_0, $\dot{\epsilon}_0$, n are experimental constants appropriate to that level. For mild steel the pair σ, $\dot{\epsilon}$ are more appropriately taken as lower yield stress and corresponding strain rate, respectively; then σ_0 has the significance of yield stress at zero strain rate. Equation (10) is capable of very good representation of observed dynamic plastic behavior

for the metals with strong strain rate sensitivity, provided strain rate history effects are negligible. Generalizations of eqn (10) are easily written, e.g. [4, 8]. These involve a yield condition, plastic strain rates being zero for stress states inside a yield surface. We adopt a simpler form derived from that of eqn (10), which is homogeneous and involves no yield condition [9]. This "matched viscous" representation replaces eqn (10) by

$$\frac{\sigma}{\sigma_0'} = \left(\frac{\dot{\epsilon}}{\dot{\epsilon}_0}\right)^{1/n'} \tag{11a}$$

where

$$\sigma_0' = \mu\sigma_0, \qquad n' = \nu n, \tag{11b}$$

with

$$\nu = \frac{1+\bar{v}_0^{1/n}}{\bar{v}_0^{1/n}}, \qquad \mu = \frac{1+\bar{v}_0^{1/n}}{\bar{v}_0^{1/\nu n}} \tag{11c}$$

and

$$\bar{v}_0 = \frac{\bar{\dot{\epsilon}}}{\dot{\epsilon}_0} \tag{11d}$$

where $\bar{\dot{\epsilon}}$ is the strain rate at which the two expressions, eqns (10) and (11a), are matched in the sense of having the same stress and slope $d\sigma/d\dot{\epsilon}$. In generalized forms, $\bar{\dot{\epsilon}}$ is the appropriate effective strain rate.

The following expressions are generalizations of eqn (11a) appropriate for general states of stress in our frame:

$$m = \frac{1}{2}\mu\{|\dot{\xi}+\dot{\eta}|^{1/n'}\,\mathrm{sgn}\,(\dot{\xi}+\dot{\eta}) + |\dot{\xi}-\dot{\eta}|^{1/n'}\,\mathrm{sgn}\,(\dot{\xi}-\dot{\eta})\} \tag{12a}$$

$$s = \frac{1}{2}\mu\{|\dot{\xi}+\dot{\eta}|^{1/n'}\,\mathrm{sgn}\,(\dot{\xi}+\dot{\eta}) - |\dot{\xi}-\dot{\eta}|^{1/n'}\,\mathrm{sgn}\,(\dot{\xi}-\dot{\eta})\} \tag{12b}$$

where

$$m = \frac{M}{M_0}, \qquad s = \frac{N}{N_0}, \qquad \dot{\xi} = \frac{\dot{\kappa}}{\dot{\kappa}_0}, \qquad \dot{\eta} = \frac{\dot{\epsilon}}{\dot{\epsilon}_0} \tag{12c}$$

$$M_0 = \frac{bH^2}{4}\sigma_0, \qquad N_0 = bH\sigma_0, \qquad \dot{\kappa}_0 = \frac{4}{H}\dot{\epsilon}_0 \tag{12d}$$

M, N being physical bending moment and axial force, respectively and $\dot{\kappa}$, $\dot{\epsilon}$ being curvature rate and axial strain rate respectively in physical terms. Although derived from a sandwich beam model [2–4], the values for pure bending and extension are either exact or extremely close to the correct values for a rectangular solid section. These constitutive equations are conservative in the sense that for a given strain rate state the stress levels are less than those in the solid section.

We next write the strain rate components in terms of velocity and displacement components in the two members AB and BC, using dimensionless variables (see eqns 9 and 12 and Fig. 2):

$$\dot{\xi}_{AB} = -\frac{1}{\alpha}\frac{L_1^2}{L_2^2}\dot{u}''_{AB}; \qquad \dot{\xi}_{BC} = -\frac{1}{\alpha}\dot{w}''_{BC} \tag{13a, b}$$

$$\dot{\eta}_{AB} = \frac{4}{\alpha}\frac{L_1^2}{L_2^2}\left(-\frac{L_2}{H}\dot{w}'_{AB} + u'_{AB}\dot{u}'_{AB}\right) \tag{13c}$$

$$\dot{\eta}_{BC} = \frac{4}{\alpha}\left(\frac{L_1}{H}\dot{u}'_{BC} + w'_{BC}\dot{w}'_{BC}\right) \tag{13d}$$

where $\alpha = 4L_1^2\dot{\epsilon}_0\tau/H^2 = (8L_1^3\dot{\epsilon}_0/H^2)\sqrt{(\rho/\sigma_0)}$ and a prime denotes differentiation with respect to y in AB and to x in BC; note that $0 \le y \le 1$, $0 \le x \le 1$. The expressions for axial strain rate in eqns (13c, 13d) contain terms where the deflection curve appears through the rotation (slope), as in the "von Karman equations" of buckling theory. They are second order correction terms, valid for deflections of moderately small size compared to the span.

The equation of energy-dissipation rate can be written for both types of frame as

$$-\frac{L_2}{L_1}\int_0^1 (\dot{u}_{AB}\ddot{u}_{AB} + \dot{w}_{AB}\ddot{w}_{AB})\,dy - \int_0^1 (\dot{u}_{BC}\ddot{u}_{BC} + \dot{w}_{BC}\ddot{w}_{BC})\,dx - k\dot{w}_1\ddot{w}_1$$

$$= \alpha\frac{L_2}{L_1}\int_0^1 (m_{AB}\dot{\xi}_{AB} + s_{AB}\dot{\eta}_{AB})\,dy + \alpha\int_0^1 (m_{BC}\dot{\xi}_{BC} + s_{BC}\dot{\eta}_{BC})\,dx \tag{14}$$

where $k = G/2\rho bHL_1$, and $\dot{w}_1 = \dot{w}_{BC}(1, t)$, $\ddot{w}_1 = \ddot{w}_{BC}(1, t)$ are velocity and acceleration of the block of mass G. When applied to the frame with attached mass, L_1 is given the reduced value 5.625 in.; for the frame without attached mass, $k = 0$ and $L_1 = 6.00$ in.

The equations of dynamics, end conditions, and equations of continuity consistent both with the kinematic forms of eqns (13) and the dissipation-energy rate equation (14) are derived as the Euler equations of the latter, the velocities and associated strain rates being treated as virtual quantities. The dynamical equations are found to be

$$m''_{AB} + 4(s_{AB}u'_{AB})' = \frac{L_2^2}{L_1^2}\ddot{u}_{AB} \tag{15a}$$

$$m''_{BC} + 4(s_{BC}w'_{BC})' = \ddot{w}_{BC} \tag{15b}$$

$$4\frac{L_2}{H}s'_{AB} = -\frac{L_2^2}{L_1^2}\ddot{w}_{AB} \tag{15c}$$

$$4\frac{L_1}{H}s'_{BC} = \ddot{u}_{BC}. \tag{15d}$$

End conditions are:

At

$$C,\quad x = 1:\quad m'_{BC}(1, t) = -k\ddot{w}_{BC}(1, t) \tag{16a}$$

$$w'_{BC}(1, t) = \dot{w}'_{BC}(1, t) = \dot{u}_{BC}(1, t) = 0. \tag{16b–d}$$

Equation (16) is recognized as the equation of motion of the attached block; k is put equal to zero for the frame without attached mass.

At

$$A,\ y = 0:\quad \dot{u}_{AB}(0, t) = \dot{u}'_{AB}(0, t) = \dot{w}_{AB}(0, t) = 0. \tag{17a–c}$$

At B, $y = 1$, $x = 0$; continuity conditions are found to be

$$\dot{u}_{AB}(1, t) = \dot{u}_{BC}(0, t);\quad \dot{w}_{AB}(1, t) = \dot{w}_{BC}(0, t) \tag{18a, b}$$

$$m_{AB}(1, t) = m_{BC}(0, t);\quad \frac{L_1}{L_2}\dot{u}'_{AB}(1, t) = \dot{w}_{BC}(0, t) \tag{18c, d}$$

$$m'_{AB}(1, t) + 4s_{AB}(1, t)u'_{AB}(1, t) - 4\frac{L_2}{H}s_{BC}(0, t) = 0 \tag{18e}$$

$$4\frac{L_1}{H}s_{AB}(1, t) + m'_{BC}(1, t) + 4s_{BC}(0, t)w'_{BC}(0, t) = 0. \tag{18f}$$

We have made the assumption, in calculations made to date, that the deformations are flexural, with unimportant effects due to lengthening or shortening of frame members. This is reasonable in view of the proportions. Hence the simplifying assumption of inextensibility was adopted, with $\dot{\eta} = 0$ in both members. The axial forces are then reactions, and eqns (12c, d) furnish relations between axial and transverse velocities:

$$\dot{w}'_{AB} = \frac{H}{L_2} u'_{AB} \dot{u}'_{AB}; \qquad \dot{u}'_{BC} = -\frac{H}{L_1} w'_{BC} \dot{w}'_{BC}. \tag{19a, b}$$

The constitutive equations then reduce to those for pure bending:

$$m_{AB} = \mu |\dot{\xi}_{AB}|^{1/n'} \operatorname{sgn} \dot{\xi}_{AB}; \qquad m_{BC} = \mu |\dot{\xi}_{BC}|^{1/n'} \operatorname{sgn} \dot{\xi}_{BC}. \tag{19a, b}$$

In the mode approximation technique we look for solutions in separated-variable form, writing

$$\dot{w}_{AB}(y, t) = \dot{w}_*(t)\phi_1(y); \qquad \dot{w}_{BC}(x, t) = \dot{w}_*(t)\phi_1(x) \tag{20a, b}$$

$$\dot{u}_{AB}(y, t) = \dot{w}_*(t)\phi_2(y); \qquad \dot{u}_{BC}(x, t) = \dot{w}_*(t)\phi_2(x) \tag{20c, d}$$

where $\phi_1 = 1$ at $x = 1$; thus $\dot{w}_* = \dot{w}_{BC}(1, t)$ is the transverse velocity at midpoint C (the major velocity magnitude). With these forms substituted in the equations of dynamics equations (15) and the kinematic relations equations (13), it may be seen that the system of equations can be split into ordinary differential equations containing either space or time variables, provided the rotation terms from the current deflection field are regarded as fixed. If these are treated as known at some stage of the response, the resulting eigen-problem can be solved to furnish the corresponding shape functions ϕ_1 and ϕ_2, and the current acceleration $\ddot{w}_*$ and velocity $\dot{w}_*$. Details of the integration by an iterative scheme are given in the Appendix. The deflection bound is determined by a closely related numerical scheme, also outlined in the Appendix.

The integration of the nondimensional equations, starting from an initial velocity field $\dot{w}^0_* \phi(x)$, can be completed once values are assigned of the parameters α, n, L_1/L_2, L_1/H, as well as of the initial velocity amplitude $\dot{w}^0_*$. (Note that μ and $n' = \nu n$ are obtained from these and the current strain rates.) The end of the motion occurs at time t^*_f such that $\dot{w}_*(t^*_f) = 0$, and the final deflection components are $w^f_* \phi_1$, $w^f_* \phi_2$. The final deflection amplitude and response time can be presented as

$$\frac{\bar{w}^f_*}{H} = w^f_* = F_1(\dot{w}^0_*, \alpha, n, L_1/H, L_1/L_2, k) \tag{21a}$$

$$\frac{\bar{t}^*_f}{\tau} = t^*_f = F_2(\dot{w}^0_*, \alpha, n, L_1/H, L_1/L_2, k) \tag{21b}$$

where we recall $\tau = 2L_1\sqrt{(\rho/\sigma_0)}$, $\alpha = (8L_1{}^3\dot{\epsilon}_0/H^2)\sqrt{(\rho/\sigma_0)}$, $k = G/2L_1\rho bH$.

Examples of plots of w^f_* and t^*_f as functions of $\dot{w}^0_*$ for various values of the material and geometrical parameters are shown in Figs. 3 and 4. The decrease of velocity amplitude to zero is illustrated in Fig. 5. The two sets of curves of Fig. 3 illustrates how the parameters α and n affect the final deflection, the remaining parameters of eqn (21) being held fixed. The curves of Fig. 4 indicate how the duration time is affected. Weak dependence on both α and n is evident. For example, multiplying α by 0.25 or 0.01 reduces the deflection by only about 10% or 50%, respectively. Figure 3(b) shows that dependence on n is similarly weak. The insensitivity to these parameters can be understood from the form of the equations. For example, the energy rate—dissipation equation based on the mode-form velocity field is

$$\ddot{w}_* \left[\int_l (\phi_1{}^2 + \phi_2{}^2)\, \mathrm{d}l + k \right] = -\left(\frac{\dot{w}_*}{\alpha}\right)^{1/n'} \frac{\mu}{2} \int_l [|\gamma + e|^{1+(1/n')} + |\gamma - e|^{1+(1/n')}]\, \mathrm{d}l \tag{22}$$

where the line integrals extend over the half-frame ABC, and

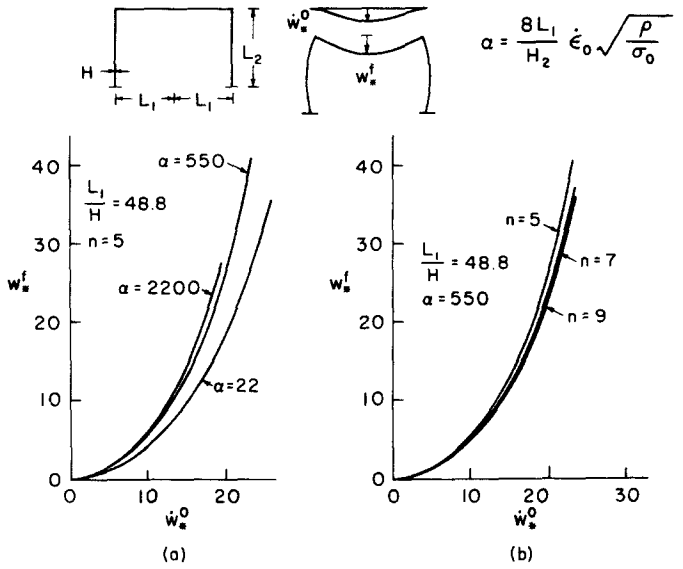

Fig. 3. Final deflection as function of initial mode form velocity (both dimensionless); (a) showing dependence on parameter α, (b) showing dependence on power n of strain rate behavior law.

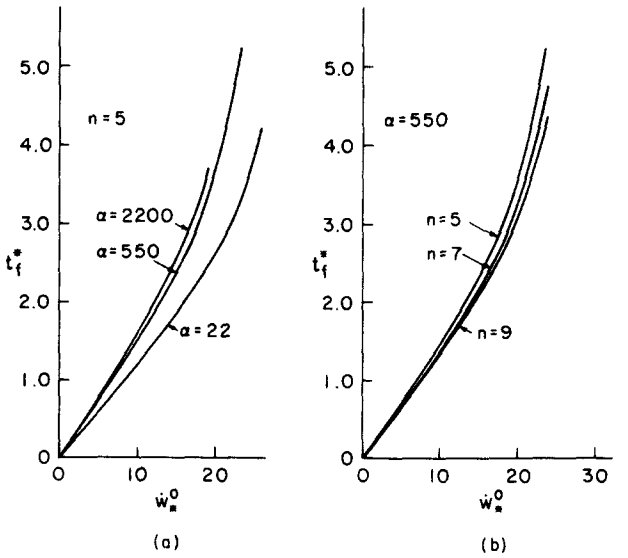

Fig. 4. Time of response as function of initial mode form velocity (both dimensionless); (a) showing dependence on parameter α, (b) showing dependence on power n of strain rate behavior law.

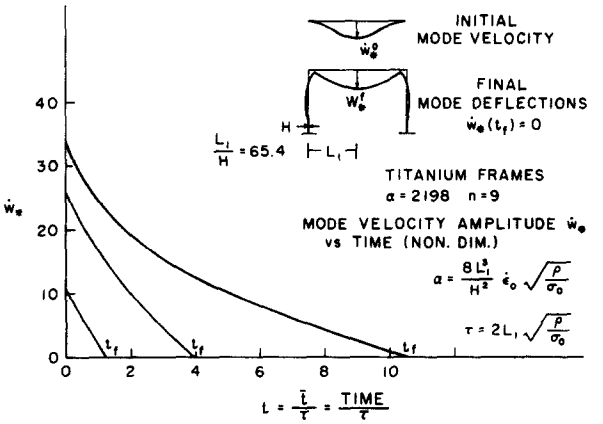

Fig. 5. Typical curves of mode velocity as function of time.

On AB:

$$\mathrm{d}l = \frac{L_2}{L_1}\mathrm{d}y, \quad \gamma = -\frac{L_1^2}{L_2^2}\phi_2'', \quad e = 4\frac{L_1^2}{L_2^2}\left(-\frac{L_2}{H}\phi_1' + u_{AB}'\phi_2'\right).$$

On BC:

$$\mathrm{d}l = \mathrm{d}x, \quad \gamma = -\phi_1'', \quad e = 4\left(\frac{L_1}{H}\phi_2' + w_{AB}'\phi_1'\right).$$

Here, as in all equations of the system, α appears only in the combination $(\dot{w}_*/\alpha)^{1/n'}$. Since $n' = \nu n$, where ν depends on current strain rate (eqn 11c) and is often approx. 2; and since n is large (5 for steel or 9 for titanium), the weak dependence on α is evident. We obtain results for a perfectly plastic material by putting $\mu = 1$, $n' \to \infty$; as expected, then the acceleration is independent of velocity and the parameter α disappears.

This insensitivity to α and n is an advantage in applications. Once the integration has been carried out for nominal values of the parameters, giving curves of w_*^f and t_f as function of $\dot{w}_*^0$ over a suitable range, these curves can be used for many particular cases of interest. For the uniform frame two such curves are shown in Fig. 6 for "steel" and "titanium", and an analogous pair of curves is shown in Fig. 7 for the frame with attached mass. An inverse procedure is used to apply these to the data of a particular test. First, the initial velocity matching formula equation (6) of the mode approximation is written (in terms of nondimensional quantities). Then from the relation between measured impulse I in physical units and the non-dimensional initial velocity $\dot{w}_c^0$, the impulse I corresponding to a particular $\dot{w}_*^0$ is obtained. Thus we obtain $\bar{w}_*^f/H$ and $t_f = \bar{t}_f/\tau$ as functions of I. The results for the two types of frames are

(a) Frame with attached mass

$$\frac{\dot{w}_*^0}{\dot{w}_c^0} = \frac{k}{\int_0^1 \phi_1^2\,\mathrm{d}x + k}; \quad \frac{I}{\dot{w}_*^0} = bH^2\sqrt{(\rho\sigma_0)}\left(\int_0^1 \phi_1^2\,\mathrm{d}x + k\right). \tag{23a, b}$$

(b) Frame with uniform beam

$$\frac{\dot{w}_*^0}{\dot{w}_c^0} = \frac{\int_0^1 \phi_1\,\mathrm{d}x}{\int_0^1 \phi_1^2\,\mathrm{d}x}; \quad \frac{I}{\dot{w}_*^0} = bH^2\sqrt{(\rho\sigma_0)}\frac{\int_0^1 \phi_1^2\,\mathrm{d}x}{\int_0^1 \phi_1\,\mathrm{d}x}. \tag{23c, d}$$

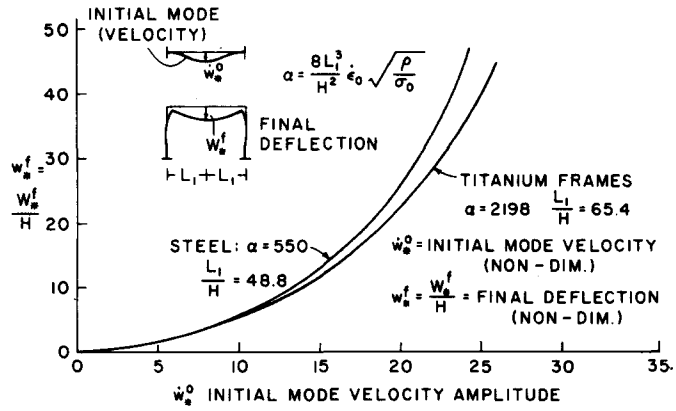

Fig. 6. "Master response curves" of final deflection-thickness ratio as function of initial mode velocity amplitude, for type (b) frames.

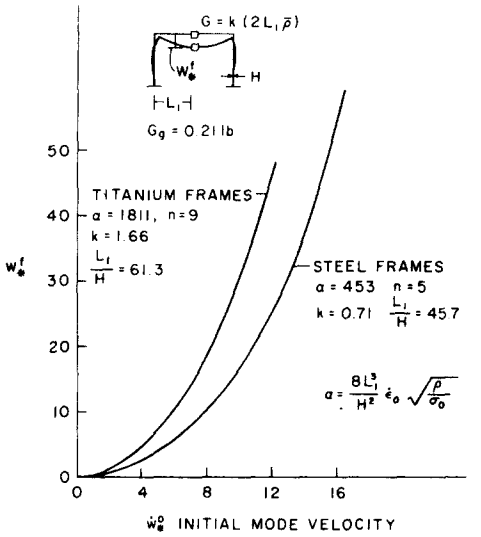

Fig. 7. "Master response curves" of final deflection-thickness ratio as function of initial mode velocity amplitude, for type (a) frames.

Taking data for the two types of frame and two materials, final deflection ratios are shown in Figs. 6 and 7 as functions of nondimensional mode velocity $\dot{w}_*^0$. From these using eqns (23b, d) are obtained curves of deflection vs impulse in physical units. Examples of such curves are given in Figs. 8–11, with points shown also from tests[1].

In computing the impulse I corresponding to a chosen value of $\dot{w}_*^0$ from eqns (23b, d), values of b, H, ρ and σ_0 appropriate for a particular test series are used, and these are used also to determine the appropriate value of the parameter $\alpha = (8L_1^3\dot{\epsilon}_0/H^2)\sqrt{(\rho/\sigma_0)}$. However in view of the insensitivity of the curves for w_*^f vs $\dot{w}_*^0$ to α, it is evident that a curve for a nominal value of α can be used for other cases. Thus the curves of Figs. 6 and 7 serve as "master response curves" for frames of a certain type of material and geometrical configuration.

To illustrate, a nominal value of α for the steel frames tested[1] may be taken as 550, corresponding to material and geometrical values in Table 1 of[1]. In particular, $\sigma_0 = 33{,}100$ psi was used, from strain rate data on the material of those tests. Thus for example, a final deflection ratio $w_*^f = \tilde{w}_*^f/H = 20$ corresponds to a nondimensional initial mode velocity $\dot{w}_*^0 = 18.0$. Using eqns (23) with $H = 0.123$ in., a final deflection of 2.46 in. is estimated to require a uniformly distributed impulse $I = 0.75$ lb-sec, as plotted in Fig. 10. Now suppose a frame of the same dimensions but of higher strength steel with $\sigma_0 = 90{,}000$ psi is to be considered. The new α would be $550\sqrt{(33.1/90)} = 334$, but the same "master curve" of Fig. 6 can be used, since the change due to a 40% reduction in α is negligible, by Fig. 3(a). Hence the impulse on the

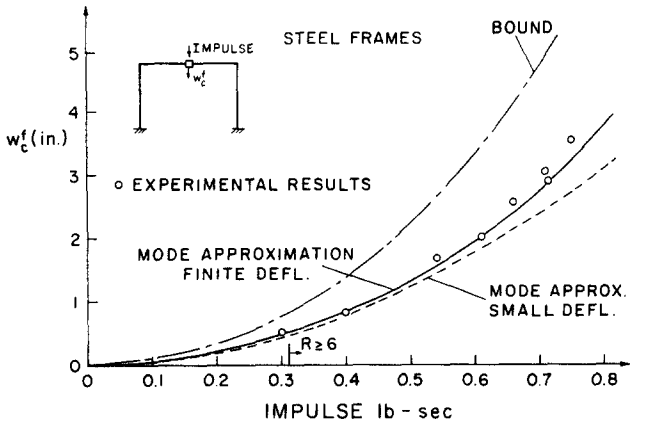

Fig. 8. Comparison of observed final midpoint deflections in tests[1] with deflection bound and predictions of mode approximation technique, for steel frames of type (a).

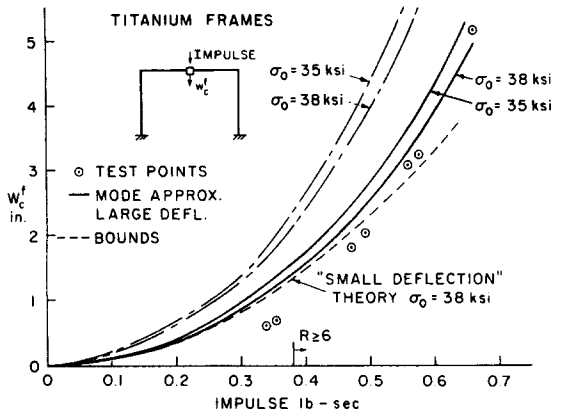

Fig. 9. Comparison of observed final midpoint deflections in tests[1] with deflection bound and predictions of mode approximation technique, for titanium frames of type (a).

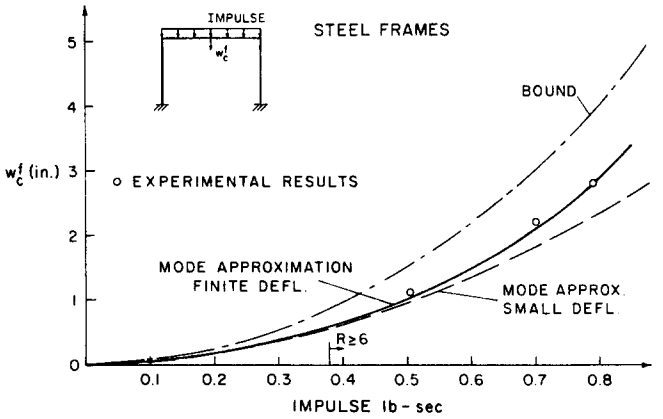

Fig. 10. Comparison of observed final midpoint deflections in tests[1] with deflection bound and predictions of mode approximation technique, for steel frames of type (b).

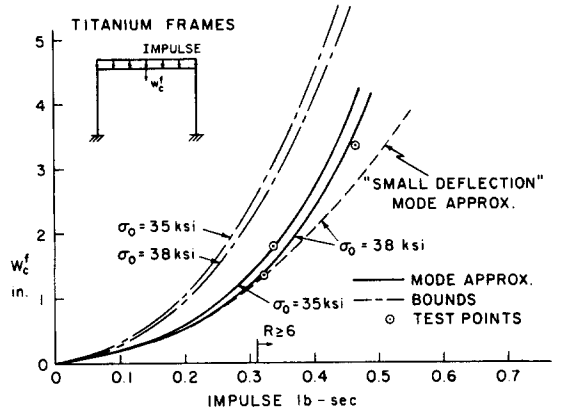

Fig. 11. Comparison of observed final midpoint deflections in tests[1] with deflection bound and predictions of mode approximation technique, for titanium frames of type (b).

stronger frame required to produce the same deflection can be estimated as $0.75\sqrt{(90/33.1)} = 1.2$ lb-sec.

This simple type of calculation was used in analyzing the tests[1] to estimate the effect of strain hardening in the titanium frames. The values of σ_0, n and $\dot{\epsilon}_0$ depend on the plastic strain at which $(\sigma, \dot{\epsilon})$ are observed in tests at nominally constant strain rate. At $\epsilon^p = 1$ and 2%, values of σ_0 were determined as 35,000 and 38,000 psi, respectively. Values of total impulse for both values are shown for the estimated deflection curves for titanium (Figs. 9 and 11). In most applications one similarly wants to explore a range of values of various parameters, including

various load distributions over the structure. It is seen that the present technique is particularly efficient for such explorations and contrasts with the typical wholly numerical approach.

3. COMPARISONS WITH TEST RESULTS

As already noted, experimental results[1] are now available for checking the estimation techniques. The basic concepts (minimum potential energy and the mode velocity matching device of eqn (6) are not in doubt, but the magnitudes of the intrinsic errors in estimates of deflections and response times are unknown. Unless these errors are reasonably small, and unless the further errors involved in implementing the techniques are also reasonably small as well as generally predictable as to sign, the methods will remain of uncertain meaning and limited usefulness. Thus the experiments are crucial for assessing the relative importance of the two classes of errors and for confirming or otherwise our expectations as to the incidental sources of error.

The deflection upper bound curves plotted in Figs. 8–11 in every case lie above the test points, indicating that the incidental errors in this calculation are either small or predominately positive. However, for the mode technique the situation is not so clear. For the concentrated impulse tests (frame type (a)) the intrinsic error is negative, since $\dot{w}_*^0 < \dot{w}_c^0$ from eqn (23a); for the uniform impulse tests (on frames of type (b)) $\dot{w}_*^0 > \dot{w}_c^0$ from eqn (23c), and the intrinsic error is positive. If all other errors were negligible, we would expect the tests points to lie *above* the estimated curves (for finite deflections) in Figs. 8 and 9, and to fall *below* them in Figs. 10 and 11. No such consistent relations are discernible in these figures. In the case of the steel frames with either concentrated or distributed loading the test points lie essentially on the estimated curve (although for concentrated impulses they tend to be consistently higher at the larger impulse magnitudes). For the titanium frames under concentrated impulses the test deflections fall well below the estimated curves, although approaching them at the larger impulse magnitudes. Under distributed impulses the titanium frames showed final deflections agreeing quite closely with the estimated curves. (For titanium two estimated deflection curves by the mode method are drawn, for two values of σ_0; as already noted, these correspond to two choices of strain level.) The fact that the experiments do not clearly show the intrinsic errors suggests that they are masked by effects of the further idealizations and approximations made in applying the mode technique. We next list these and consider them briefly.

(1) A "rigid-viscoplastic" theory was used: elastic deformations were neglected (elastic moduli taken as infinite). Here we are considering strongly rate sensitive metals so that stress levels are raised and elastic strains probably increased in importance. On the simplest basis, we may suppose that the energy ratio R of initial kinetic energy to total elastic strain energy capacity must exceed about 6 for an error of less than 15% in the permanent deflection; this takes over a result[10] derived from a one-degree-of-freedom model and seems conservative for perfectly plastic behavior. The values of impulse required for $R \geq 6$ are indicated in Figs. 8–11. If the same results held for the present rate sensitive materials there would appear to be some correlation between this (arbitrary) criterion for the neglect of elastic deformations and the experimental discrepancies. In the one case where the criterion is not satisfied in some of the tests, namely the concentrated impulse tests on titanium frames shown in Fig. 9, the test points at the smaller impulse magnitudes fall considerably below the estimated deflection curves, but approach them as the impulse is increased. Note that for this case the intrinsic error is negative (the test points should lie above the estimated curve in the absence of other errors); hence the effect of elastic deflections would be even larger than indicated.

As already noted, errors due to elastic effects may be larger when the material is strongly rate sensitive than indicated by the criterion applied, as above, for perfectly plastic behavior. The omission of elastic deformations makes for substantial simplification, but further basic research is needed to determine what errors are likely to be caused by it. It should probably be regarded here as a major suspect.

(2) The constitutive equations express plastic strain rates as explicit functions of stresses, with implicit account of strain hardening through the experimental constants. If the arbitrarily chosen plastic strain level is low (or if the lower yield stress is used rather than a fixed strain level), equations of this type would underestimate strain hardening and hence lead to overestimates of deflections. However, as illustrated for the titanium frames, it is easy to deduce

deflection estimates based on a larger magnitude of plastic strain, and thus to take account of strain hardening.

(3) Strain rate history effects were neglected, the experimental constants being obtained from tests at nominally constant strain rates. The influence of prior strain rate history has been studied mainly by tests in which the strain rate is rapidly increased[11]. A few tests involving a rapid decrease have been described[12]; these would be more directly relevant to the present response histories, where the structure is set in motion in a very short time, after which the strain rates decrease to small values, perhaps roughly monotonically. On the basis of various hypotheses to account for observed history effects, in particular the use of plastic work as a state variable[13] and dynamic recovery[14], one would expect strain rate history effects in the present case to lead to positive errors, i.e. to cause the test specimens to deflect less than the estimated value. The data are quite limited, but there seems little reason to expect that such errors would be important here.

(4) Constitutive equations of homogeneous viscous type (without yield condition) were used, derived from inhomogeneous forms based directly on strain rate test data. The matching formula used (eqns 11c) is such that the stress levels are lower, at the same strain rate, than those according to the more realistic forms. Hence over-estimates of deflections are again expected. The errors due to this device have been very small in the examples worked to date[3, 9]. Experience is limited, but there seems no reason to expect large errors in the present cases.

(5) The deformation is assumed to remain flexural at large deflections, with axial forces treated as reactions. Expressions for center-line strain rate in terms of transverse and axial velocity components are of second order accuracy (product of rotation by rotation rate). Setting the axial strain rate equal to zero furnishes relations between the velocity components, involving the transverse deflection.

The errors due to the use of approximate strain expressions at finite displacements, and to the assumption of zero net center-line strain rate are difficult to assess as to magnitude or sign. The second order terms are those widely used in approximate theories of buckling, but are clearly valid only in a range of "moderately large" deflections. At final deflections approaching a third of the span, this representation is questionable. The treatment of axial forces as reactions which do not contribute to the energy dissipation rate implies a certain over-estimate of local strength. However it does not seem possible from this to argue how the final deflections will be affected. Intuitively we feel that the errors due to these aspects are not serious ones, but further investigation is necessary.

(6) The pressure pulse is idealized as "impulsive", delivering finite impulse in vanishingly small time. It is well known that this idealization leads to over-estimates of major deflections[15] when applied to rigid-perfectly plastic structures using small deflection equations. The error in the over-estimate in those cases can be shown to be given approximately by the ratio of the pulse duration to the duration of motion of the structure. These results certainly do not apply exactly to problems where visco-plastic and large deflection effects are important. However in the present problems the pulse duration is very short compared to the response time of the structure (roughly 10 μsec compared to 10 msec), and the resulting error is believed to be positive but of minor importance.

(7) The integration technique used to obtain final deflections of the structure with initial mode form velocity employed "instantaneous mode" solutions at a sequence of times, each such solution corresponding to the current deflection field. They are linked by proper differential relations only at one point of the structure, where the major velocity and deflection magnitudes occur. Hence although current field equations are satisfied, some continuity conditions are disregarded. Extremal theorems are available for the small-small equations[7, 16]. These can be applied to the current state and show that the mode form velocity field renders the energy dissipation rate an extremum among all kinematically admissible fields with the same kinetic energy. Here the extremum is a minimum, and the theorem characterizes the mode form solution as minimizing the rate of decrease of kinetic energy, for a fixed level of kinetic energy. The error in using this technique is therefore inferred to be positive.

(8) Apart from the basic approximation in treating the actual motion as a sequence of

instantaneous modes, the determination of current mode shapes and accelerations involves solving a nonlinear eigenproblem by numerical means. This was done by an iterative scheme, as outlined in the Appendix. The numerical scheme made use of a subdivision of the column and half-span into 100 elements. It furnishes an essentially exact solution at low cost. No difficulties with convergence were met at any deflection magnitudes, and it is believed that negligible errors are introduced in this part of the response calculation.

The simplifications discussed above are involved in both the deflection bound and the mode technique, with the exception of (7) which obviously refers only to the latter approach. It may be noted that in the numerical evaluation of the deflection bound, the iterative scheme used for determining the deflected shape under static loading has common ground with that used in the numerical solution of the eigen-problem of the extended mode technique.

It is seen that the errors that can be identified with the idealizations and approximations as listed are mainly positive, i.e. such as to cause too large a deflection. The exceptional cases are items (5) and (8), where no statements on the sign of the error seem tenable. In some cases, for example the neglect of elastic deformation and of strain rate history effects, the arguments are somewhat conjectural. This seems unavoidable at the present stage.

The comparison of test results with the large deflection bounds indicates that the method of calculation of the bounds is satisfactory. However, their comparison with large deflections predicted by the mode technique shows inconsistencies. In the tests with uniform impulse where the intrinsic error is positive, as are most of the other errors, the estimated deflection curve should lie distinctly above the test points; the actual test points lie essentially on the curves (Figs. 10 and 11). In the tests with concentrated impulse, the intrinsic error is negative. This is shown clearly by the results for steel frames in Fig. 8, which suggests that the other errors are small by comparison. However, the results for the titanium frames in Fig. 9 are then anomalous, since to explain them the incidental errors must be large. Here perhaps the influence of elastic deformations is more important as indicated by the energy ratio criterion.

Test results are given in[1] for measures of response time, and for the inward deflection at the top of each column; this secondary deflection is zero in a "small-deflection" theory. The present theory gives quite good agreement in both cases.

In conclusion, the present work has illustrated the application to large deflections of an impulsively loaded viscoplastic structure of bound and mode estimation techniques. The efficiency of both techniques compared to purely numerical approaches has been emphasized. Comparisons with fairly comprehensive experimental results[1] have validated the deflection bound calculation, but have shown up inconsistencies in the estimates of final deflections by the extended mode technique. These demonstrate the need for further study of the approximations made in implementing this method. Despite this, it is worth emphasizing that the estimated deflections by the extended mode method in most cases agree extremely well with the final deflections observed in the tests. In the one test series where the discrepancies are large (Fig. 9), the estimates are conservative (actual permanent deflections are smaller); these occur in circumstances of relatively small final deflections where elastic deflections are more important. Hence there seems no doubt that practical use can be made of this approach, with normal caution.

REFERENCES

1. S. R. Bodner and P. S. Symonds, Experiments on impulsively loaded plane frames of mild steel and titanium. *Int. J. Solids Structures* **15**, 1–13 (1978).
2. P. S. Symonds and C. T. Chon, Bounds for finite deflections of impulsively loaded structures with time dependent plastic behavior. *Int. J. Solids Structures* **11**, 403–423 (1975).
3. P. S. Symonds and C. T. Chon, Approximation techniques for impulsive loading of structures of time-dependent plastic behavior with finite deflections. *Proc. Oxford Conf.* Mechanical properties of materials at high strain rates. Inst. of Physics Conf. (Edited by J. Harding). Ser. No. 21, pp. 299–315 (December 1974).
4. C. T. Chon and P. S. Symonds, Large dynamic deflection of plates by mode method. *J. Engng Mech. Div., Proc. ASCE* **103**(EM1), 3–14 (1977).
5. J. B. Martin and P. S. Symonds, Mode approximations for impulsively loaded rigid-plastic structures. *J. Engng Mech. Div., Proc. ASCE* **92**(EM5), 43–66 (1966).
6. J. B. Martin, A note on uniqueness of solutions for dynamically loaded rigid-plastic and rigid-viscoplastic continua. *J. Appl. Mech.* **33**, 207–209 (1966).
7. P. S. Symonds and T. Wierzbicki, On an extremum principle for mode form solutions in plastic structural dynamics. *J. Appl. Mech.* **42**(3), 630–640 (1975).

8. P. Perzyna, The constitutive equations for rate sensitive plastic materials. *Q. Appl. Math.* **20**, 321–331 (1963).
9. P. S. Symonds, Approximation techniques for impulsively loaded structures of rate sensitive plastic behavior. *SIAM J. Appl. Math.* **25**(3), 462–473 (1973).
10. P. S. Symonds, Survey of methods of analysis for plastic deformation of structures under dynamic loading. *Rep. BU/NSRDC/1–67*, from Brown University to Office of Naval Research, Naval Ship Research and Development Center, Contract Nonr 3248(01)(X) (June 1967).
11. R. A. Frantz, Jr. and J. Duffy, The dynamic stress–strain behavior of torsion of 1100–0 aluminum subjected to a sharp increase in strain rate. *J. Appl. Mech.* **39**(4), 939–945 (1972).
12. J. Lipkin and J. D. Campbell, Strain rate history effects in dynamic shear. *Euromech* 83 *Colloquium on Dynamic Response of Plastic Structures and Continua*, Mátrafüred, Hungary, 1–3 November 1976. See report by N. Jones, *Int. J. Mech. Sci.* **19**, 125–128 (1977).
13. S. R. Bodner and Y. Partom, Dynamic inelastic properties of materials: Part II—Representation of time dependent characteristics of metals. ICAS Paper No. 72-28, *8th Cong. Int. Council of the Aeronautical Sciences.* International Congrescentrum Rai-Amsterdam, The Netherland, pp. 9–14 (28 August–2 September 1972).
14. J. Klepaczko and J. Duffy, Strain rate and temperature memory effects for some polycrystalline fcc metals. Conf. Series No. 21, The Institute of Physics, *Mechanical Properties at High Rates of Strain*, pp. 91–101 (1974).
15. C. K. Youngdahl, Correlation parameters for eliminating the effect of pulse shape on dynamic plastic deformation. *J. Appl. Mech.* **37**, 744–752 (1970).
16. J. B. Martin Extremum principles for a class of dynamic rigid-plastic problems. *Int. J. Solids Structures* **8**, 1185–1204 (1972).
17. L. S. S. Lee, Mode responses of dynamically loaded structures. *J. Appl. Mech.* **39**, 904–910 (1972).

APPENDIX

The iterative scheme used to determine the instantaneous mode at each time stage in the *mode technique* is essentially the same as that used in the solution for finite deflections of a circular plate[4]. It is noteworthy that the deflection function giving the deflection bound can be obtained by the same iteration scheme. We shall sketch briefly how the equations of the two problems can be put in analogous form, omitting most of the details.

Equations only for the transverse member BC will be written, for brevity. We look first at the mode technique. When the modal forms of eqns (20) are used, the dimensionless bending moment in the transverse member BC can be written as

$$m = \mu \left(\frac{\dot{w}_*}{\alpha}\right)^{1/n'} |-\phi_1''|^{1/n'} \operatorname{sgn}(-\phi_1''). \tag{A1}$$

Equations (19b), (15d) and (15b) can be integrated with respect to x and put in the following forms:

(19b)
$$\phi_2' = -\frac{H}{L_1} w' \phi_1' \tag{A2}$$

(15d)
$$s = \ddot{w}_* \left[\frac{H}{4L_1} \int_0^x \phi_2 \, dx + s_0\right] \tag{A3}$$

$$\mu \left(\frac{\dot{w}_*}{\alpha}\right)^{1/n'} [|-\phi_1''|^{1/n'} \operatorname{sgn}(-\phi_1'')]' + 4sw' = \ddot{w}_* \left[\int_0^x \phi_1 \, dx + A\right]. \tag{A4}$$

Here s_0 and A are constants and the prime denotes differentiation with respect to x, position in member BC measured from B. (All quantities refer to this member, but subscripts are omitted.) Similar equations can be written for member AB, and the boundary conditions include fixing at A and C, continuity at B, and the normalizing condition $\phi_1 = 1$ at C. After use of eqn (A3), eqn (A4) can be written as

$$\operatorname{sgn}(-\phi_1'')(|-\phi_1''|^{1/n'})' = \Lambda \left\{\int_0^x \phi_1 \, dx + A - 4w' \left[\frac{H}{4L_1} \int_0^x \phi_2 \, dx + S_0\right]\right\} \tag{A5}$$

where

$$\Lambda = \ddot{w}_* / \mu \left(\frac{\dot{w}_*}{\alpha}\right)^{1/n'}.$$

Integrating eqn (A2), we obtain

$$\phi_2 = -\frac{H}{L_1} \left[\int_0^x w' \phi_1' \, dx - \int_0^1 w' \phi_1' \, dx\right]. \tag{A6}$$

At any stage of the response the slope function $w'(x)$ can be estimated from the field at a preceding stage together with the velocity and acceleration fields at that stage. Admissible shape functions $\phi_1(x)$ in BC and $\phi_2(\bar{y})$ in AB can also be guessed, satisfying the stated conditions at A, B and C; the functions for the preceding stage may be used, except at $t = 0$. Equation (A6) then furnishes $\phi_2(x)$ in BC, apart from integration constants. With use of the analogous equations for AB and the fixing, continuity, and normalization conditions, all of the integration constants can be determined, and new shape functions obtained. From each set of functions the quantity Λ (eqn A5) can be computed from the energy rate-dissipation equation (14), which takes the form

$$\Lambda = -\frac{\int_0^1 |-\phi_1''|^{1+(1/n')} \, dx + \frac{L_2}{L_1} \int_0^1 |-\phi_2''|^{1+(1/n')} \, dy}{\int_0^1 (\phi_1^2 + \phi_2^2) \, dx + \frac{L_2}{L_1} \int_0^1 (\phi_1^2 + \phi_2^2) \, dy + k}. \tag{A7}$$

Cycles of iteration may be terminated when the magnitude Λ reaches a steady value. From the final values, the velocity and displacement fields can be written, and approximate functions for a subsequent instant obtained.

At the start, $w' = 0$ and $\dot{w}_*^0$ is chosen arbitrarily, with guessed admissible functions $\phi_2(y)$ and $\phi_1(x)$ in AB and BC, respectively. The response terminates at $\dot{w}_*(t_f) = 0$, final deflections being obtained by interpolation when $\dot{w}_*$ first becomes negative.

The *deflection bound* requires only one determination of shape functions over the frame, rather than functions at a sequence of times during the response as in the mode technique. To obtain an upper bound on the final deflection of the midpoint C of the frame, a force P is applied at this point. If the work done quasi-statically by this force in time t_f is not less than K_0, where t_f is the actual response time and K_0 the given initial kinetic energy, then the deflection corresponding to this force is an upper bound on the same component of deflection resulting from the given initial velocities.

Use of minimum work paths to fixed final strains at time t_f [2, 3] for the material behavior represented by eqns (11, 12) enables us to write moment-curvature relations

$$\dot{\kappa} t_f = \kappa^f = \dot{\kappa}_0 t_f \left| \frac{n'}{n'+1} \frac{M}{\mu M_0} \right|^{n'} \operatorname{sgn} M^f \tag{A8}$$

where κ^f and M^f are curvature and moment at time t_f, respectively. Nondimensional stresses may be defined as

$$\bar{m} = \left[\frac{t_f}{\tau}\right]^{1/n'} \frac{n'}{n'+1} \frac{M^f}{M_0}; \quad \bar{s} = \left[\frac{t_f}{\tau}\right]^{1/n'} \frac{n'}{n'+1} \frac{N^f}{N_0} \tag{A9}$$

where $\tau = 2L_1\sqrt{(\rho/\sigma_0)}$ is the reference time used also in the mode method. The equation of equilibrium for the beam member BC with a concentrated force P at L_1, written as a delta function, is

$$M'' + (Nw)' = -\frac{P}{2}\delta(x - L_1). \tag{A10}$$

This may be integrated once, and with nondimensional variables as in eqns (9) and (A9) the four equations for this member can be written as

$$\bar{m}' + 4\bar{s}w' = \bar{p} \tag{A11a}$$

$$\bar{m} = \mu \left| \frac{\kappa^f}{\dot{\kappa}_0 \tau} \right|^{1/n'} \operatorname{sgn} \kappa^f = \mu \left| -\frac{1}{2} w'' \right|^{1/n'} \operatorname{sgn}(-w'') \tag{A11b}$$

$$\bar{s} = \bar{C}_1 = \text{const.} \tag{A11c}$$

$$u = -\frac{1}{2}\frac{H}{L_1}(w')^2 \tag{A11d}$$

where

$$p = \left(\frac{t}{\tau}\right)^{1/n} \frac{L_1 P}{2M_0}, \quad \text{and} \quad \alpha = 8L_1{}^3\dot{\epsilon}_0\sqrt{(\rho/\sigma_0)}/H^2.$$

The analogous equations for AC, and the boundary and continuity equations, are omitted for brevity. The work-kinetic energy condition eqn (1b) takes the form

$$\frac{K_0}{M_0} \leqslant 2\mu\alpha \frac{H}{L_1}\left(\frac{t_f}{\tau}\right)^{1/n'}\left[\int_0^1 \left|\frac{\bar{m}}{\mu}\right|^{n'+1} dx + \frac{L_2}{L_1}\int_0^1 \left|\frac{\bar{m}}{\mu}\right|^{n'+1} dy\right]. \tag{A12}$$

In these equations, the response time t_f appears explicitly only in eqn (A12), because of the definitions of $\bar{m}$ and $\bar{p}$. The inequality shows that t_f, which is unknown, may be replaced by an upper bound t_f^u. We shall not attempt to derive an exact upper bound. Note that t_f appears only as $t_f^{1/n'}$, where n' is large (e.g. 10), so results are insensitive to t_f. For small deflections and rigid-perfectly plastic behavior, upper bounds on the response time for the present frame problems can be obtained by Lee's method [17] and written as

$$t_f^u = \eta \frac{\bar{\rho} L_1{}^2 V_0}{4M_0} \tag{A13}$$

where $\eta = 2k\sqrt{(1 + 1/3k)}$ for type (a) frames (attached mass and concentrated impulse) and $\eta = 2/\sqrt{3}$ for type (b) frames. The effect of finite deflections is to lengthen, while that of strain rate sensitivity is to shorten the response time. Hence while the expressions for t_f^u are not exact for our conditions, they are probably more than adequate.

It is convenient to write the deflection field in the form

$$w = D\phi_1(x) \text{ in } BC; \quad w = D\phi_1(y) \text{ in } AB \tag{A14a}$$

$$u = D\phi_2(x) \text{ in } BC; \quad u = D\phi_2(y) \text{ in } AB \tag{A14b}$$

where D is the dimensionless displacement at the midpoint C of the beam member. An iteration scheme is started by giving D an arbitrary value, e.g. $D = 20$, and assuming numerical functions $\phi_1(x)$ in BC and $\phi_2(y)$ in AB. Equations such as eqn (A11d) then furnish the corresponding axial components $\phi_2(x)$ in BC and $\phi_1(y)$ in AB. The equations of equilibrium (e.g. eqn A11a), together with the moment-curvature equations (e.g. eqn A11b), can now be written entirely in terms of the

transverse shape functions $\phi_1(x)$ and $\phi_2(y)$ and their derivatives, so that from starting functions new functions are obtained by quadratures, with constants of integration which must be found from the boundary and continuity equations. The forms of the equations are identical with those in the mode method, with different meaning of the constants.

The experiments with which we have made comparisons involve direct measurements of the total impulse (I) applied to the frame. Thus for the two frame types

$$\text{(a)}\quad I = GV_0, \quad K_0 = \frac{1}{2}GV_0^2 = \frac{I^2}{2G} = \frac{I^2}{4k\rho bHL_1} \tag{A15a}$$

$$\text{(b)}\quad I = 2L_1\bar{\rho}V_0, \quad K_0 = L_1\bar{\rho}V_0^2 = \frac{I^2}{4L_1\bar{\rho}} = \frac{I^2}{4\rho bHL_1}. \tag{A15b}$$

Using these and the expressions for the upper bound on response time, eqn (A13), we have relations between impulse and midpoint deflection ratio $D = w_c^f/H$ as follows

$$\text{Type (a):}\quad \left(\frac{I^2}{kb^2H^3L_1\rho\sigma_0}\right)^{1+(1/2n')} = 2\mu\frac{H}{L_1}D\left(\frac{16kHD^2}{\eta^2L_1\alpha^2}\right)^{(1/2n')}\psi[\phi_1''(x), \quad \phi_2''(y)] \tag{A16a}$$

$$\text{with}\quad \eta = 2k\sqrt{(1+1/3k)}, \quad k \approx G/2L_1\rho bH$$

$$\text{Type (b):}\quad \left(\frac{I^2}{b^2H^3L_1\rho\sigma_0}\right)^{1+(1/2n')} = 2\mu\frac{H}{L_1}D\left(\frac{12HD^2}{L_1\alpha^2}\right)^{(1/2n')}\psi[\phi_1''(x), \quad \phi_2''(y)] \tag{A16b}$$

where (for both types)

$$\psi[\phi_1''(x), \quad \phi_2''(y)] = \int_0^1 |-\phi_1''(x)|^{1+(1/n')}\,dx + \frac{L_2}{L_1}\int_0^1 |-\phi_2''(y)|^{1+(1/n')}\,dy. \tag{A16c}$$

Suitable values of $\mu = \sigma_0'/\sigma_0$ and $\nu = n'/n$ are obtained from the initial strain rates by means of eqn (11). The initial mode form velocity field, with magnitude $\dot{w}_*^0$ derived from given initial velocity or impulse values through the mode matching technique of eqn (6), may be used with $\phi(x)$ and $\phi(y)$ determined as outlined above. This field gives initial maximum curvature rates and strain rates which, of course, are not the actual initial strain rates, but are smoothed values that are appropriate for present purposes.